



RESEARCH ARTICLE OPEN ACCESS

Dealing with Missing Angular Sections in NanoCT Reconstructions of Low Contrast Polymeric Samples Employing a Mechanical *In Situ* Loading Stage

Rafaela Debastiani^{1,2}  | Chantal Miriam Kurpiers³ | Enrico Domenico Lemma^{4,5,6} | Ben Breitung^{1,2} | Martin Bastmeyer^{4,7} | Ruth Schwaiger⁸  | Peter Gumbsch^{1,9,10}

¹Institute of Nanotechnology, Karlsruhe Institute of Technology, Karlsruhe, Germany | ²Karlsruhe Nano Micro Facility (KNMFi), Eggenstein-Leopoldshafen, Germany | ³Institute for Applied Materials - Mechanics of Materials and Interfaces, Karlsruhe Institute of Technology, Eggenstein-Leopoldshafen, Germany | ⁴Zoological Institute, Karlsruhe Institute of Technology, Karlsruhe, Germany | ⁵Department of Engineering, Università Campus Bio-Medico of Rome, Rome, Italy | ⁶Institute of Nanotechnology (NANOTEC), National Research Council, Lecce, Italy | ⁷Institute of Biological and Chemical Systems - Biological Information Processing, Karlsruhe Institute of Technology, Eggenstein-Leopoldshafen, Germany | ⁸Institute of Energy and Climate Research - Microstructure and Properties of Materials (IEK-2), Forschungszentrum Jülich, Jülich, Germany | ⁹Institute for Applied Materials - Reliability and Microstructure, Karlsruhe Institute of Technology, Karlsruhe, Germany | ¹⁰Fraunhofer Institute for Mechanics of Materials IWM, Freiburg, Germany

Correspondence: Rafaela Debastiani (rafaela.debastiani@kit.edu)

Received: 26 January 2024 | **Revised:** 26 July 2024 | **Accepted:** 10 November 2024

Review Editor: Alberto Diaspro

Funding: This work was supported by Deutsche Forschungsgemeinschaft, Alexander von Humboldt-Stiftung.

Keywords: *in situ* imaging | *in situ* mechanical testing | limited angle | low contrast samples | nanoCT | X-ray microscope

ABSTRACT

While *in situ* experiments are gaining importance for the (mechanical) assessment of metamaterials or materials with complex microstructures, imaging conditions in such experiments are often challenging. The lab-based computed tomography system Xradia 810 Ultra allows for the *in situ* (time-lapsed) mechanical testing of samples. However, the *in situ* loading setup of this system limits the image acquisition angle to 140°. For low contrast polymeric materials, this limited acquisition angle leads to regions of low information gain, thus preventing an accurate reconstruction of the data using a filtered back projection algorithm resulting in erroneous microstructures. Here, we demonstrate how the information gain can be improved by selecting an appropriate position of the sample. A low contrast polymeric tetrahedral microlattice sample and a structured sample with specific markers, both scanned over 140° and 180°, demonstrate that the missing structural details in the 140° reconstruction are limited to an angular wedge of about 20°. Depending on the sample geometry and microstructure, applying simple strategies for the *in situ* experiments allows accurate reconstruction of the data. For the tetrahedral microlattice, a simple rotation of the sample by 90° rotates all relevant surfaces by about 30° to the original illumination direction, creating a more even X-ray illumination for all the projections, thus providing enough X-ray absorption for an accurate reconstruction of the geometry.

1 | Introduction

In situ experiments are increasingly important for the understanding of materials behavior and properties. Combining different experiments with X-ray computed tomography allows for the

study of internal structural changes in a specimen as a function of time and applied stimulus. Among standard environmental setups integrated with X-ray imaging are heating devices (Saif et al. 2019; Shearing et al. 2011) and mechanical loading devices (Daemi et al. 2019; Dall'Ara et al. 2022; Peña Fernández

This is an open access article under the terms of the [Creative Commons Attribution-NonCommercial](https://creativecommons.org/licenses/by-nc/4.0/) License, which permits use, distribution and reproduction in any medium, provided the original work is properly cited and is not used for commercial purposes.

© 2024 The Author(s). *Microscopy Research and Technique* published by Wiley Periodicals LLC.

Summary

- The effects of limited acquisition angle in X-ray computed tomography on the reconstruction using a filtered back projection algorithm were studied systematically.
- Erroneous interpretation of microstructures, in particular of complex materials with low absorption contrast, can be avoided by proper alignment of the sample.

et al. 2021; Sommerschuh et al. 2021; Sykes et al. 2019). X-ray computed tomography (CT) configurations vary in terms of sample size, imaging resolution and tomography acquisition speed. These CT parameters determine the kind of phenomena that can be observed in *in situ* experiments (Withers et al. 2021). For laboratory-based X-ray computed tomography, the acquisition of a complete tomography may take several hours, and thus *in situ* experiments are well suited to study processes that can be monitored in a time-lapsed manner, such as the formation of cracks upon stepwise loading (Patterson et al. 2016). For faster processes such as liquid metal foaming and sub-micron resolution, currently only synchrotron sources offer the required X-ray flux for the acquisition of hundreds of tomograms per second (García-Moreno et al. 2019).

The laboratory-based transmission X-ray microscope Xradia 810 Ultra (nanoCT) offers the possibility of mechanical *in situ* testing under indentation, uniaxial compression or tension. Imaging is possible with a resolution down to 50 nm in absorption and Zernike phase contrast modes. While it is a great opportunity for imaging specimens under load with high resolution in a lab-based system, this particular setup also imposes a few limitations such as the maximum field of view of 65 μm and a limited angle of 140° for the projections acquisition using the *in situ* load stage. With the load stage at a fixed position, the sample rotation has to be carried out between -70° and $+70^\circ$. The remaining $\pm 20^\circ$ are shadowed by the anvil.

Filtered back projection (FBP) is the most commonly used analytical algorithm to reconstruct computed tomography data (Withers et al. 2021) and the base for the Zeiss proprietary software Scout and Scan Reconstructor. Typically, the FBP reconstruction is based on the acquisition of 2D projections collected with equal angle increments over 180° or more. For each projection angle, the detector collects X-ray photographs of the sample. In the case of the nanoCT, which has a parallel beam geometry, each row of the detector can be reconstructed independently. The back projection algorithm then projects evenly the intensity of the X-ray photons collected by the detector along the angle in which it was recorded. With the collection of projections at different angles, the different projections intersect, thereby reconstructing the image of an object. Due to the uneven sampling at the center and at the edges of an object, the final back projection image is blurry. Applying a filter (e.g., ramp filter) to the projections suppresses the low frequency components in the Fourier space, compensating for the high frequency components missing due to the insufficient sampling, thus creating a sharper image. The reconstruction with FBP presents some limitations such as noise and image artifacts. Acquiring projections over a

range smaller than 180°, as it happens when using the *in situ* load stage in the Xradia Ultra nanoCT, can result in areas of missing information in the reconstructed 3D image using FBP (Withers et al. 2021; Schofield et al. 2020). Such missing information is particularly critical for samples with regions of low X-ray absorption.

In this article, we systematically evaluated the inaccuracy in the reconstruction data of low absorption contrast samples scanned over a limited angle range using the nanoCT Xradia 810 Ultra equipped with the *in situ* load stage setup. Two polymeric specimens of different geometries were used to demonstrate the effect of such a missing angular wedge in the reconstruction. A correct positioning of the sample facilitates the collection of sufficient information to obtain an accurate reconstruction.

2 | Materials and Methods

2.1 | Sample Preparation

Two samples denoted as samples A and B were printed using 3D direct laser writing (3D-DLW—Photonic Professional PPGT2, Nanoscribe GmbH) using IP-Dip resin (Nanoscribe GmbH). To avoid further manipulation of the samples, the polymeric samples were printed directly on the titanium pin of the *in situ* load stage.

For sample A, a tetrahedral microlattice geometry (Figure 1a) was chosen and printed with a laser power of 10.6 mW and a printing speed of 3000 $\mu\text{m}/\text{s}$ as described in (Kurpiers, Hengsbach, and Schwaiger 2021). In addition, three bars were added to the geometry sticking out on the side of the sample (marked by arrows in Figure 1a) to serve as markers for the nanoCT scan. Sample B was a more uniform sample, created as a 50 μm diameter cylinder composed of vertical plates with a width 3 μm and different symbols at the end of the plates (Figure 1b). Here, the laser power was 25 mW and the scanning speed 5000 $\mu\text{m}/\text{s}$ and further developed as described in (Lemma et al. 2022).

After sample B was first scanned in the nanoCT, it was coated with a layer of Al_2O_3 to enhance the contrast and scanned again. The coating was deposited by Atomic Layer Deposition (ALD) using a Picosun R-200 Advanced system. A 100 nm thick alumina layer was prepared from trimethylaluminum (TMA) and H_2O at 130°C in 1750 cycles.

2.2 | NanoCT

Samples A and B were scanned using the lab-based transmission X-ray microscope Zeiss Xradia 810 Ultra, referred to as nanoCT, for the acquisition of their 3D reconstruction. This system operates with a rotating Cr-anode (energy of 5.4 keV) and the samples in the current study were scanned in a field of view corresponding to 65 μm and pixel size of 128 nm. Absorption and Zernike phase contrast modes were employed to scan the samples using 901 and 1601 projections.

In order to understand the effects of angular range and the regions of low information gain when using the *in situ* loading setup provided by Zeiss (Figure S1), experiments were performed with both

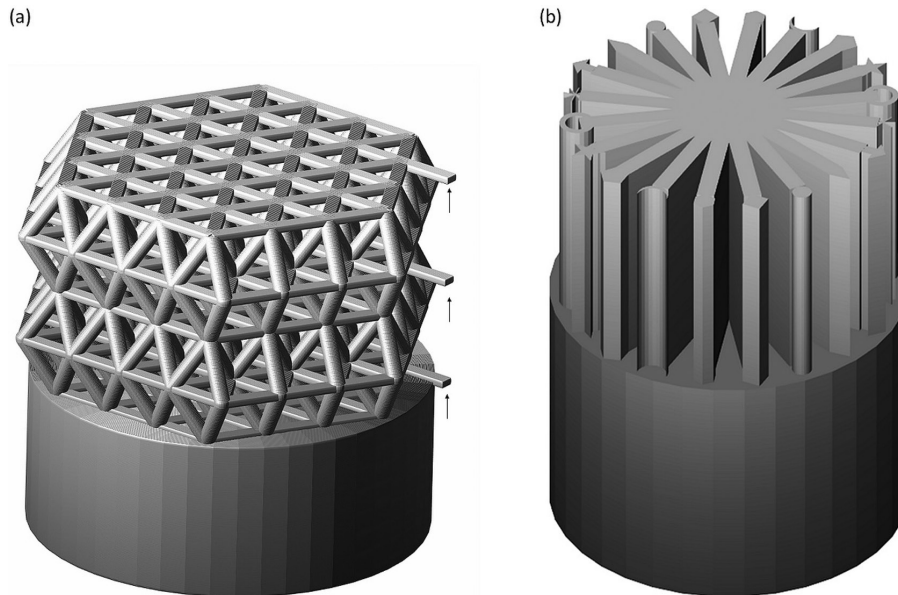


FIGURE 1 | 3D models of the samples. (a) Sample A (diameter of $60\ \mu\text{m}$), a tetrahedral microlattice geometry with 3 bars sticking out on the side, indicated by arrows, to serve as markers for the nanoCT scan. (b) Sample B (diameter of $50\ \mu\text{m}$), a cylindrical uniform sample with plates and different symbols at the end of the plates.

the standard (Figure S2) and *in situ* setup. The standard scan was carried out over 180° (maximum angle of projection acquisition in this system), from -90° to $+90^\circ$, while the *in situ* scan was carried out from -70° to $+70^\circ$ (over 140°). In addition, the sample position for sample A was rotated to 45° and 90° (Figure 3a—pen mark on the side of the pin), with 0° corresponding to the typical sample positioning. Sample B was scanned at 0° and 90° . With the rotation, we aimed to verify the influence of the X-ray illumination of different parts of the sample on the data reconstruction when dealing with limited angle of scanning.

The projections were 3D reconstructed using the proprietary Zeiss Scout and Scan Control System Reconstructor (version 13.08) software, which is available with the equipment and is based on the filtered back projection algorithm. The reconstructed data was visualized using the ORS Dragonfly software (Dragonfly, Dragonfly ORS 2022).

3 | Results

Using the mechanical *in situ* load stage for experiments in the nanoCT, the projection acquisition limited to 140° may cause the absence of sample information during the reconstruction. We observed such incorrect reconstruction in metamaterials. For example, the reconstruction of sample A scanned using the *in situ* setup showed the sample as defective, with the absence of the “horizontal beams” (Figure 2a). If sample A is scanned in the standard sample stage over 180° , the complete sample can be reconstructed (Figure 2b). This indicates that the missing beams were the result of the limited angle of acquisition and the weak X-ray absorption in such structures.

To improve the resolution at the reduced angular scanning range of 140° we increased the number of projections from 901 to 1601. This did not alter the reconstruction results. Rotating

the sample to illuminate different angles with respect to the microstructure (Figure 3) improved the results. The XY views for the sample placed in 0° (typical position), 45° and 90° with respect to the anvil and scanned in phase and absorption contrast modes are shown in Figure 3. We found that turning the sample to 45° gives a better reconstruction compared to 0° . With the sample positioned at 90° , the reconstruction of all beams is equivalent to the scan over 180° (Figure 2b).

For a better visualization of the difference in the reconstruction of the absorption contrast scans, a $5\ \mu\text{m}$ line was drawn in a corresponding “horizontal beam” (Figure 4a) and the grayscale values were plotted as a function of the line distance (Figure 4b). The grayscale distribution in the reconstruction of the samples scanned over 180° and over 140° at position 90° are similar, with an expect increase in the intensity in the region corresponding to the “horizontal beam”. For the sample scanned over 140° at position 0° and 45° , the grayscale shows a small variation over the measured distance. The grayscale intensity values for the samples scanned over 180° and over 140° at position 90° vary about 23.000 between the background and the “horizontal beams” regions, while for the reconstructions of the scans over 140° at positions 0° and 45° , are mostly uniform with grayscale values varying approximately 9.000 and 7.000, respectively.

With the aim of specifically characterizing the regions of the sample with lower information gain, sample B was scanned over 140° in the positions 0° and 90° with respect to the anvil. The results shown in Figure 5 demonstrate that the sample was only partially reconstructed. The region not reconstructed corresponds to an angular range of approximately 20° . In this specimen, the regions not directly illuminated by the X-ray beam due to the limited angle of projection acquisition are located on the left and right side of the sample. When rotating the sample by 90° , plates that were not reconstructed are now visible (symbols marked with a red circle in Figure 5a,b).

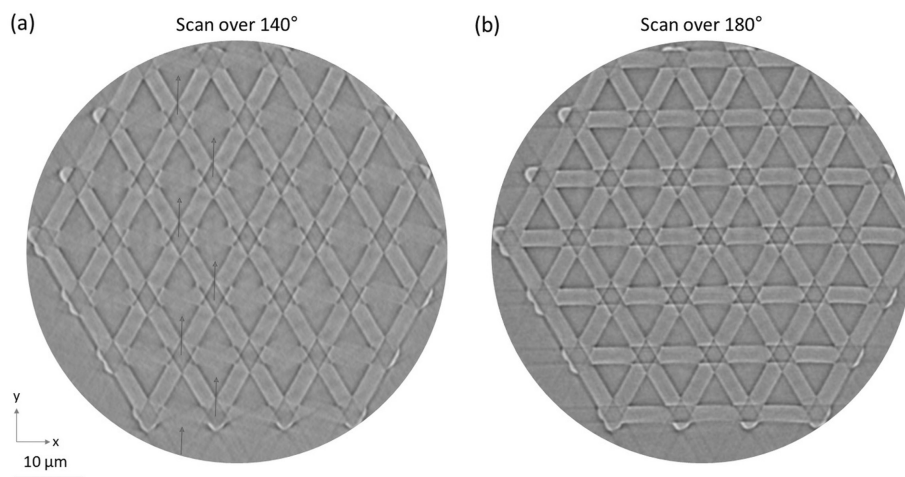


FIGURE 2 | XY view of (a) Sample A scanned from -70° to $+70^\circ$ (projections acquired over 140°). Arrows indicate the horizontal missing beams rows. (b) Sample A scanned from -90° to $+90^\circ$ (projection acquired over 180°). Both samples were scanned in Zernike phase contrast mode and reconstructed using the software Zeiss Scout and Scan Control System Reconstructor. The diamonds (a) and stars (b) in the nodes of the structure are reconstruction artifacts.

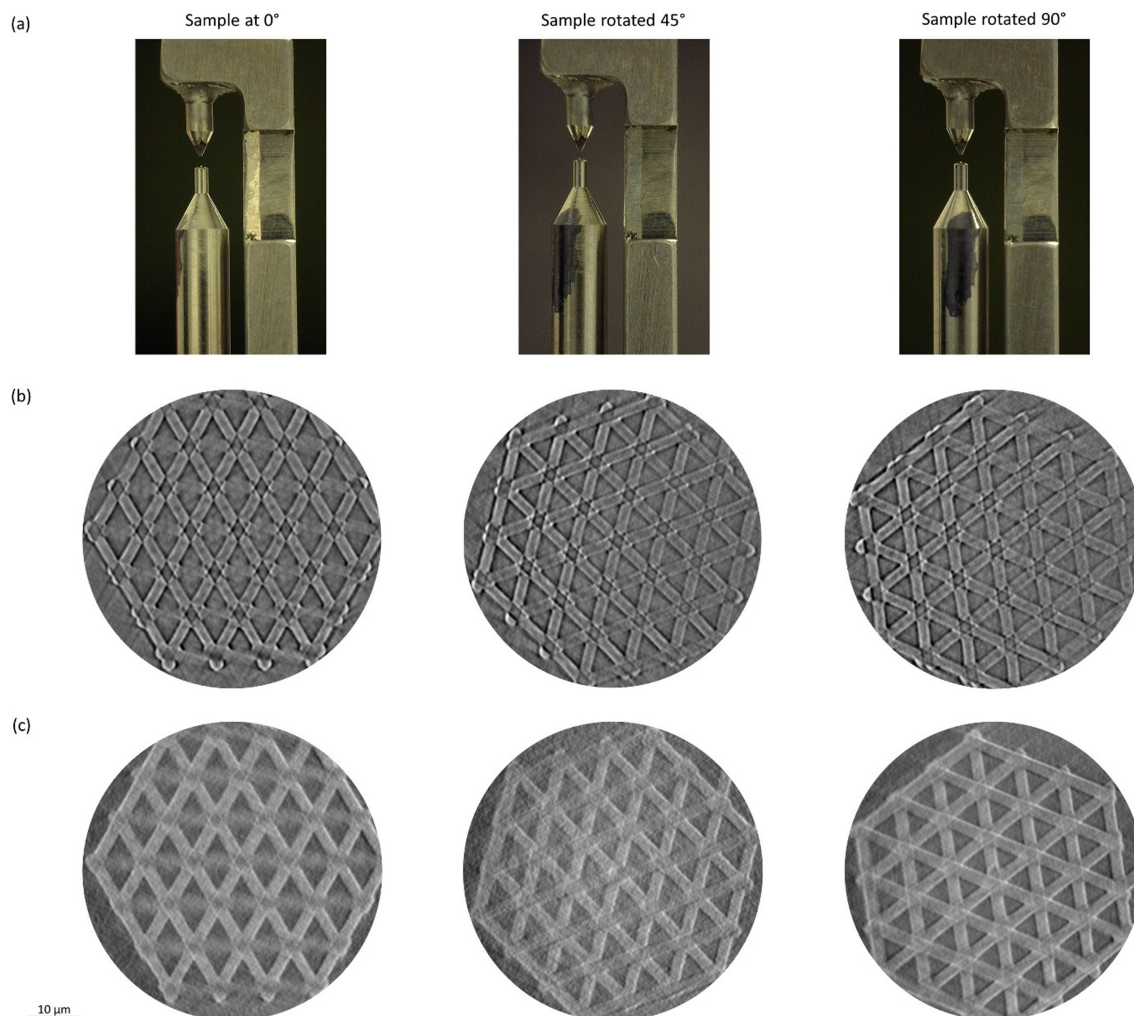


FIGURE 3 | (a) Position of the sample on the pin in relation to the anvil in the load stage (pen marking), corresponding to the typical position (0°) and the pin rotated 45° and 90° . XY views of sample A scanned from -70° to $+70^\circ$ with the sample placed into different angles in the stage, in Zernike phase contrast (b) and absorption contrast (c).

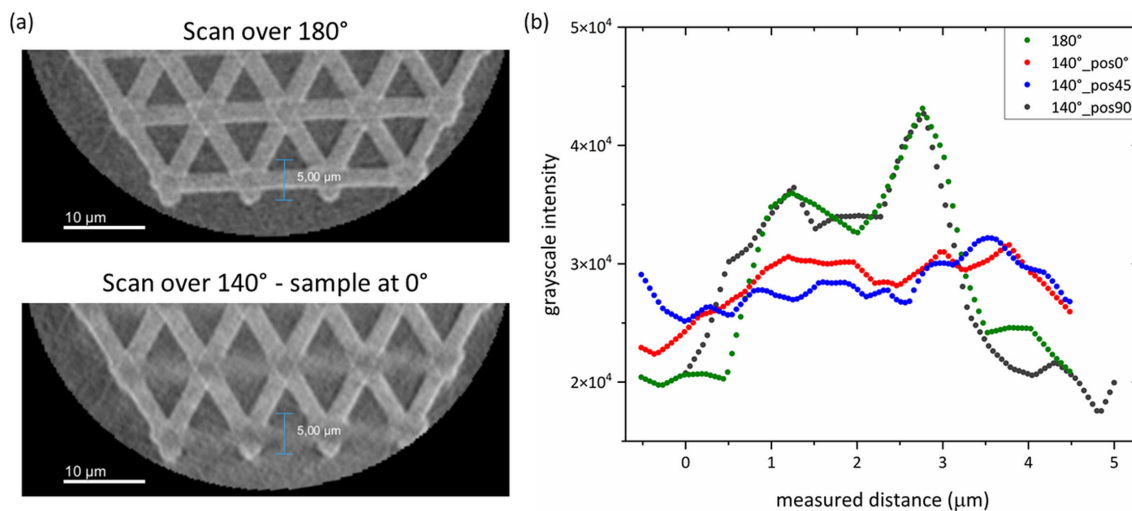


FIGURE 4 | (a) XY view of the sample scanned in absorption contrast over 180° and 140° with the sample positioned at 0°. A 5 μm line was drawn in a “horizontal beam” to extract the grayscale values of the region. (b) Grayscale values distribution plotted as a function of the measuring distance from (a). Scans with an accurate reconstruction create a peak of grayscale distribution, while the scans with missing “horizontal beams” have a more uniform distribution of values.

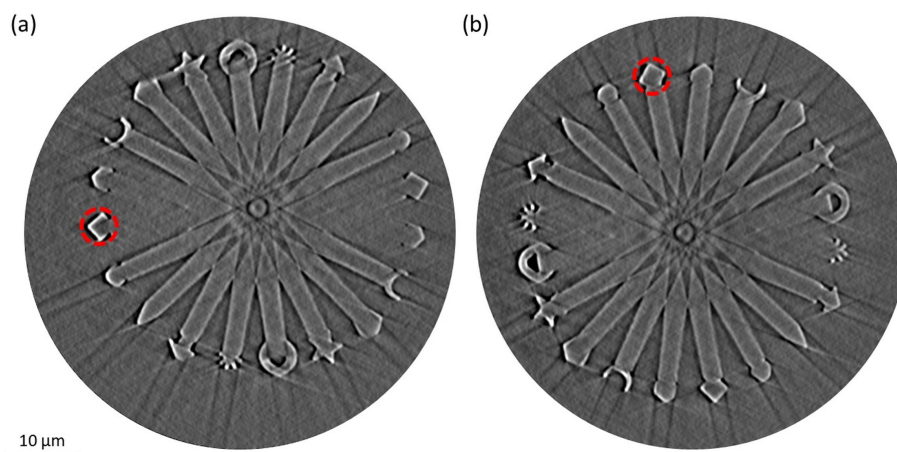


FIGURE 5 | Sample B scanned over 140° positioned at 0° (a) and 90° (b) with respect to the anvil. The bars that are oriented in a certain angular position are not reconstructed, while the symbols are visible. The plate not visible in (a) (marked with a red circle) is visible when rotating the sample in 90°. These reconstructions are made from phase contrast imaging.

In order to evaluate the influence of the density of the sample in such a setup, sample B was coated with 100 nm of Al₂O₃. Figure 6 shows that the coating led to an improved reconstruction of the sample. While in the polymeric sample two bars are missing in the reconstruction (Figure 6a,c), in the coated sample only one bar is not fully reconstructed (Figure 6b,d).

4 | Discussion

The low contrast of polymeric structures or metamaterials combined with the limited angle of scan imposed by the mechanical *in situ* load stage of the Xradia 810 Ultra causes the suppression of data during the reconstruction (Figure 2). The missing 40° sector of scanning range leads to an angular range of about 20° in which the surfaces within the structures or other weak contrast features are blurred or completely invisible. This happens for both absorption contrast and Zernike phase contrast (Figure 3) and cannot be improved by increasing the number

of scans within the limited angle range of 140°. It is important to note that the missing angular wedge is not an effect of direct “shadowing” by the anvil but of the missing low angle illumination in certain directions combined with the low contrast of the polymer. This can be concluded from the remaining visibility of the symbols at the end of the missing bars in the poorly reconstructed region of the sample (Figure 5) and from the lack of visibility of the horizontal bars in the lattice structure (Figure 2). Due to the low contrast of the polymeric sample, the illumination at only large angles apparently is insufficient to reconstruct bars in the missing illumination directions. This suggests two possible routes along which the reconstruction problem might be tackled. First, one can attempt to enhance contrast by coating the sample and second one can try to avoid the alignment of structural features for example in lattice structures or metamaterials within this missing angular space.

Increasing the absorption contrast of the polymeric materials by coating them with 100 nm of Al₂O₃ was indeed sufficient to

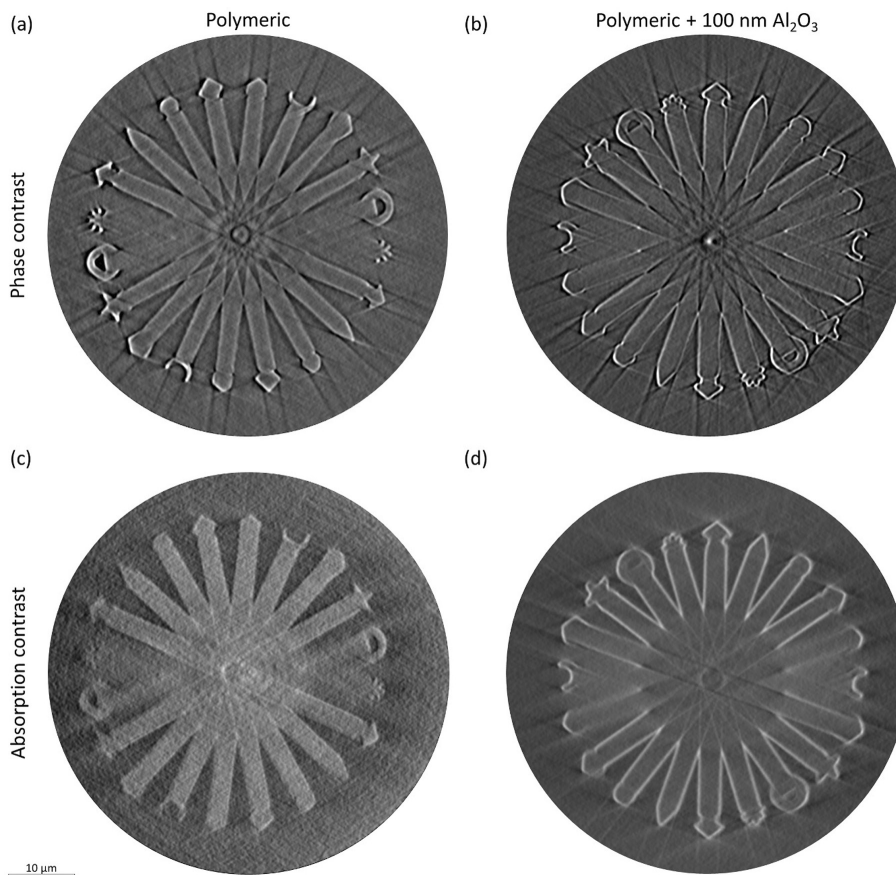


FIGURE 6 | Sample B scanned over 140° in Zernike phase contrast (a and b) and absorption contrast (c and d) before (left—a and c) and after (right—b and d) coating the sample with 100 nm of Al_2O_3 . The coating increased the contrast and improved the reconstruction, although did not eliminate the problem, as one of the plates is still not reconstructed.

increase the contrast significantly. The absorption length for the X-ray energy of 5.4 keV for Al_2O_3 is $25\ \mu\text{m}$, while it is about 16 times larger (Ravel and Newville 2005) for the IP-Dip photoresist ($\text{CH}_2\text{N}_{0.001}\text{O}_{0.34}$, solid density $1.2\ \text{g}/\text{cm}^3$) (Stein et al. 2018), corresponding to an absorption depth of $416.8\ \mu\text{m}$. The thin coating improves reconstruction results but does not completely eliminate the problem as one plate is still not reconstructed in Figure 6. Furthermore, coating a sample of course changes its mechanical properties (Schroer, Wheeler, and Schwaiger 2018) and therefore this is not really an option for most *in situ* mechanical testing experiments.

Metamaterials and other artificially structured materials are often built from beams or plates composed into lattice structures or geometrically simple building blocks (Estrin et al. 2021). In many cases, like in our example sample A, the elements are connected at angles larger than 45° . This leaves an angular space in the structure to which no surfaces and no structural elements are aligned. The horizontal missing beams in sample A correspond to the directions of the missing X-ray illumination during the limited angle scan. Rotating the sample by 90° rotates all relevant surfaces by about 30° to the original illumination direction. This creates a more even X-ray illumination for all the projections and leads to a complete reconstruction of the data, which is almost as good as for a complete 180° scan.

5 | Conclusions

Dealing with *in situ* setups may impose limitations on tomography experiments. Using the mechanical load stage for *in situ* imaging in the lab-based X-ray microscope Xradia 810 Ultra implies scanning the samples over a limited angle of 140° . Although for many specimens this limitation does not interfere with the reconstruction of the data using a filtered back projection algorithm, it is a problem in particular for samples whose structures are not known, as the limited angle tomography can lead to an erroneous reconstruction and thus predict materials features, that either do not exist or will be overlooked. The limited acquisition angle is absolutely critical for low contrast, polymeric structures and particularly for microlattices at certain angular positions. Due to the geometry and low contrast of the polymeric microlattices, parts of the sample (the “horizontal beams”) are not reconstructed. Increasing the contrast of the sample through a thin layer of Al_2O_3 improves the reconstruction significantly but of course modifies the sample properties.

To resolve this issue in lattice structures without modifying the sample is to rotate the sample to an angle that allows for a more even X-ray illumination of the internal surfaces and avoiding beam orientations parallel to the missing angular wedge of the illumination. Accurate reconstruction of our tetrahedral sample

was possible despite the limited angular scanning range when the sample was scanned at such position.

For such low contrast polymeric structures scanned over a limited acquisition angle, as is the case of the *in situ* load stage at the Xradia Ultra X-ray microscope, it is therefore advisable to scan the sample over both the complete 180° and the limited 140° range of the *in situ* setup before actually starting the *in situ* experiment to make sure that all relevant structural elements are visible. This experimental workflow reduces the inaccuracies in the scan reconstruction and avoids additional experiments and analysis steps.

Author Contributions

Rafaela Debastiani: conceptualization, investigation, writing – review and editing, data curation, writing – original draft, methodology, project administration, validation, visualization, formal analysis. **Chantal Miriam Kurpiers:** methodology, conceptualization, investigation, writing – review and editing, validation, visualization. **Enrico Domenico Lemma:** investigation, writing – review and editing. **Ben Breitung:** investigation, writing – review and editing. **Martin Bastmeyer:** resources, supervision. **Ruth Schwaiger:** supervision, conceptualization, writing – review and editing, funding acquisition, methodology, validation. **Peter Gumbsch:** supervision, writing – review and editing, conceptualization, funding acquisition, methodology, validation.

Acknowledgments

This work was partly carried out with the support of the Karlsruhe Nano Micro Facility (KNMF, www.knmf.kit.edu), a Helmholtz Research Infrastructure at Karlsruhe Institute of Technology (KIT, www.kit.edu). The Xradia 810 Ultra (nanoCT) core facility was supported (in part) by the 3DMM2O—Cluster of Excellence (EXC-2082/1390761711). R.D., C.M.K., E.D.L., M.B., R.S and P.G. acknowledge the support by the Cluster of Excellence 3DMM2O (EXC_2082/1-390761711) funded by the German Research Foundation (DFG). The work of E.D.L. has been supported by a postdoctoral research fellowship of the Alexander von Humboldt Foundation, and by the Italian Ministry for University and Research (Young Researchers - Seal of Excellence, CUP C83C22001250006).

Conflicts of Interest

The authors declare no conflicts of interest.

Data Availability Statement

The data that support the findings of this study are available from the corresponding author upon reasonable request.

References

Daemi, S. R., X. Lu, D. Sykes, et al. 2019. “4D Visualisation of In Situ Nano-Compression of Li-Ion Cathode Materials to Mimic Early Stage Calendering.” *Materials Horizons* 6: 612–617. <https://doi.org/10.1039/c8mh01533c>.

Dall’Ara, E., A. J. Bodey, H. Isaksson, and G. Tozzi. 2022. “A Practical Guide for In Situ Mechanical Testing of Musculoskeletal Tissues Using Synchrotron Tomography.” *Journal of the Mechanical Behavior of Biomedical Materials* 133: 105297. <https://doi.org/10.1016/j.jmbbm.2022.105297>.

Dragonfly, Dragonfly ORS. 2022. <http://www.theobjects.com/dragonfly>.

Estrin, Y., Y. Beygelzimer, R. Kulagin, et al. 2021. “Architecturing Materials at Mesoscale: Some Current Trends.” *Materials Research Letters* 9: 399–421. <https://doi.org/10.1080/21663831.2021.1961908>.

García-Moreno, F., P. H. Kamm, T. R. Neu, et al. 2019. “Using X-Ray Tomoscopy to Explore the Dynamics of Foaming Metal.” *Nature Communications* 10: 3762. <https://doi.org/10.1038/s41467-019-11521-1>.

Kurpiers, C. M., S. Hengsbach, and R. Schwaiger. 2021. “Architectural Tunability of Mechanical Metamaterials in the Nanometer Range.” *MRS Advances* 6: 507–512. <https://doi.org/10.1557/s43580-021-00094-1>.

Lemma, E. D., Z. Jiang, F. Klein, et al. 2022. “Adaptation of Cell Spreading to Varying Fibronectin Densities and Topographies Is Facilitated by $\beta 1$ Integrins.” *Frontiers in Bioengineering and Biotechnology* 10: 964259. <https://doi.org/10.3389/fbioe.2022.964259>.

Patterson, B. M., N. L. Cordes, K. Henderson, et al. 2016. “In Situ Laboratory-Based Transmission X-Ray Microscopy and Tomography of Material Deformation at the Nanoscale.” *Experimental Mechanics* 56: 1585–1597. <https://doi.org/10.1007/s11340-016-0197-3>.

Peña Fernández, M., A. P. Kao, R. Bonithon, et al. 2021. “Time-Resolved In Situ Synchrotron-microCT: 4D Deformation of Bone and Bone Analogues Using Digital Volume Correlation.” *Acta Biomaterialia* 131: 424–439. <https://doi.org/10.1016/j.actbio.2021.06.014>.

Ravel, B., and M. Newville. 2005. “ATHENA, ARTEMIS, HEPHAESTUS: Data Analysis for X-Ray Absorption Spectroscopy Using IFEFFIT.” *Journal of Synchrotron Radiation* 12: 537–541. <https://doi.org/10.1107/S0909049505012719>.

Saif, T., Q. Lin, Y. Gao, et al. 2019. “4D In Situ Synchrotron X-Ray Tomographic Microscopy and Laser-Based Heating Study of Oil Shale Pyrolysis.” *Applied Energy* 235: 1468–1475. <https://doi.org/10.1016/j.apenergy.2018.11.044>.

Schofield, R., L. King, U. Tayal, et al. 2020. “Image Reconstruction: Part 1 – Understanding Filtered Back Projection, Noise and Image Acquisition.” *Journal of Cardiovascular Computed Tomography* 14: 219–225. <https://doi.org/10.1016/j.jcct.2019.04.008>.

Schroer, A., J. M. Wheeler, and R. Schwaiger. 2018. “Deformation Behavior and Energy Absorption Capability of Polymer and Ceramic-Polymer Composite Microlattices Under Cyclic Loading.” *Journal of Materials Research* 33: 274–289. <https://doi.org/10.1557/jmr.2017.485>.

Shearing, P. R., R. S. Bradley, J. Gelb, et al. 2011. “Using Synchrotron X-Ray Nano-CT to Characterize SOFC Electrode Microstructures in Three-Dimensions at Operating Temperature.” *Electrochemical and Solid-State Letters* 14: B117. <https://doi.org/10.1149/1.3615824>.

Sommerschuh, M., J. Wirth, S. Englisch, et al. 2021. “A Scale-Bridging Study of the Influence of TCP Phases on the Mechanical Properties of an Additive Manufactured Ni-Base Superalloy Combining Microcompression Testing, X-Ray Nanotomography and TEM.” *Microscopy and Microanalysis* 27: 938–942. <https://doi.org/10.1017/S1431927621003603>.

Stein, O., Y. Liu, J. Streit, et al. 2018. “Fabrication of Low-Density Shock-Propagation Targets Using Two-Photon Polymerization.” *Fusion Science and Technology* 73: 153–165. <https://doi.org/10.1080/15361055.2017.1406237>.

Sykes, D., R. Hartwell, R. S. Bradley, et al. 2019. “Time-Lapse Three-Dimensional Imaging of Crack Propagation in Beetle Cuticle.” *Acta Biomaterialia* 86: 109–116. <https://doi.org/10.1016/j.actbio.2019.01.031>.

Withers, P. J., C. Bouman, S. Carmignato, et al. 2021. “X-Ray Computed Tomography.” *Nature Reviews Methods Primers* 1: 18. <https://doi.org/10.1038/s43586-021-00015-4>.

Supporting Information

Additional supporting information can be found online in the Supporting Information section.